Modifying ADAMTS13 to modulate binding of pathogenic autoantibodies of patients with acquired thrombotic thrombocytopenic purpura

Nuno A. G. Graça,[1,2] Bogac Ercig,[2,3,4] Leydi Carolina Velásquez Pereira,[5] Kadri Kangro,[5] Paul Kaijen,[2] Gerry A. F. Nicolaes,[3,4] Agnès Veyradier,[6,7] Paul Coppo,[7-9] Karen Vanhoorelbeke,[5] Andres Männik[1] and Jan Voorberg[2]

[1]Icosagen Cell Factory OÜ, Õssu, Kambja, Tartumaa, Estonia; [2]Department of Molecular and Cellular Hemostasis, Sanquin-Academic Medical Center Landsteiner Laboratory, Amsterdam, the Netherlands; [3]Pharmatarget, Maastricht, the Netherlands; [4]Department of Biochemistry, Cardiovascular Research Institute Maastricht (CARIM), Maastricht University, Maastricht, the Netherlands; [5]Laboratory for Thrombosis Research, IRF Life Sciences, KU, Leuven Campus Kulak Kortrijk, Kortrijk, Belgium; [6]Service d'Hématologie Biologique and EA3518–Institut Universitaire d'Hématologie, Groupe Hospitalier Saint Louis-Lariboisière, AP-HP, Université Paris Diderot, Paris, France; [7]Centre de Référence des Microangiopathies Thrombotiques, Hôpital Saint-Antoine, AP-HP, Paris, France; [8]Service d'Hématologie, Hôpital Saint-Antoine, AP-HP, Paris, France and [9]Sorbonne Université, UPMC Université Paris, Paris, France

 doi:10.3324/haematol.2019.226068

Received: May 8, 2019.

Accepted: November 21, 2019.

Pre-published: November 21, 2019.

Correspondence: *JAN VOORBERG* - j.voorberg@sanquin.nl

Supplementary Materials & Methods

Modifying ADAMTS13 to modulate binding of pathogenic autoantibodies of patients with acquired thrombotic thrombocytopenic purpura

Authors: Nuno A. G. Graça[1,2], Bogac Ercig[2,3,4], Leydi Carolina Velásquez Pereira[5], Kadri Kango[5], Paul Kaijen[2], Gerry A. F. Nicolaes[3,4], Agnès Veyradier[6,8], Paul Coppo[7-9], Karen Vanhoorelbeke[5], Andres Männik[1] and Jan Voorberg[2]

Running Title: ADAMTS13 variants that escape autoantibodies in iTTP

Scientific Section: THROMBOSIS AND HEMOSTASIS

Affiliations:

[1]Icosagen Cell Factory OÜ, Õssu, Kambja, Tartumaa, Estonia

[2]Department of Molecular and Cellular Hemostasis, Sanquin-Academic Medical Center Landsteiner Laboratory, Amsterdam, The Netherlands

[3]Pharmatarget, Maastricht, The Netherlands

[4]Department of Biochemistry, Cardiovascular Research Institute Maastricht (CARIM), Maastricht University, 6200 MD Maastricht, The Netherlands.

[5]Laboratory for Thrombosis Research, IRF Life Sciences, KU, Leuven Campus Kulak Kortrijk, Kortrijk, Belgium

[6]Service d'hématologie biologique and EA3518-Institut universitaire d'hématologie, Groupe Hospitalier Saint Louis-Lariboisière, AP-HP, Université Paris Diderot, 2 rue Ambroise Paré, 75010, Paris, France

[7]Service d'Hématologie, Hôpital Saint-Antoine, AP-HP, Paris, France

[8]Centre de Référence des Microangiopathies Thrombotiques, Hôpital Saint-Antoine, AP-HP, Paris, France

[9]Sorbonne Université, UPMC Univ Paris 06, Paris, France

Statement of Prior Presentation: *Partially presented as an oral communication at the 9th Bari International Conference, Rome, IT, September 17, 2017 and presented at the 10th Bari International Conference, Genoa, IT, September 8, 2019.*

Rationale for amino-acid choice for each panel of mutations

The entire collection of exosite-3 RFRYY epitope variants used in this study is shown in **Figure 1**. We present here the rationale behind the choices of mutations made for this study. The degree of residue conservation was taken into account, taking a further step from the rationale used by Jian *et al*. to build the classic GoF variant[4]. One amino-acid was chosen to represent the different degrees of conservation based on the amino-acids side-chain structures and their general physicochemical properties. In the classic GoF variant, aromatic residues within this epitope (F592, Y661 and Y665) were mutated to other closely-resembling aromatic residues. In this case the closest aromatic residue from phenylalanine is tyrosine and vice-versa. The arginines were changed to the only other positively-charged amino-acid available (lysine)[4]. In our 'Conservative panel', we opted to follow a similar approach, without changing the arginines (Y↔F), but we introduced the mutations individually and then cumulatively in all possible combinations within these three aromatic residue positions. We opted for this approach because it is known that a positive charge is necessary in residue 660 to maintain ADAMTS13 activity[5]. Next, we sought to introduce progressively less conservative mutations with different properties from those conferred by alanine. Of all the 20 amino-acids available, the amino-acid with no aromatic ring that resembled phenylalanine and tyrosine the closest was considered by us to be leucine, which retains hydrophobic properties. This yielded a panel of 'Semi-Conservative' variants (Y/F→L). Next we attempted to introduce polarity into this epitope without directly introducing positive or negative charges. Of all available polar amino-acids, asparagine has the most similar structure with leucine, and this was our amino-acid of choice to yield a panel of 'Non-Conservative' variants (Y/F→N). In this case, care was taken to not introduce a putative N-glycosylation site. A panel of alanine substitutions of the aromatic residues was included because alanines have been used before in autoantibody binding studies, however not in full-length context[2]. Alanine substitutions of arginines alone or together with aromatic residues were also included to comprehensively scrutinize the contributions of each amino-acid in this epitope (Y/F/R→A). An extra panel of alanine replacements of the aromatic residues together with arginine substitutions by lysine (alanine/lysine hybrids) were included

because previous studies demonstrate that the positive charges here are also important for the binding of antibodies[2,6], yet are simultaneously crucial for the proteolytic activity of ADAMTS13[2,5].

DNA constructs and ADAMTS13 mutation insertions

Full-length ADAMTS13 wild-type (1427 aa), truncated ADAMTS13 wild-type spanning from the metalloprotease domain to the spacer domain ('MDTCS') and an MDTCS variant containing 5 alanine mutations in the spacer exosite-3 (R568A/F592A/R660A/Y661A/Y665A) (each with 685 aa) have been described previously[1,2]. For protein production, we used mammalian CHO cells employing QMCF technology (European Patent EP1851319B1, www.icosagen.com)[3]. The cDNAs of all ADAMTS13 variants described above and below were cloned into plasmid expression vector pQMCF3 (Icosagen Cell Factory OÜ). All cDNAs were tagged at the C-terminal end with a V5 epitope followed by a 6xHis-tag (see **supplementary Figure 1**). Briefly, panels of spacer exosite-3 mutants were designed with conservative mutations[4], semi-conservative mutations with leucine, non-conservative mutations with asparagine (no putative N-glycosylation sites were introduced), and alanine mutations (**Figure 1 and Supplementary Table 2**). Leucine and asparagine were chosen as replacement residues based on the physicochemical properties of the side-chain. Most of these panels maintained R568 and R660 intact. In some cases, these arginines were also mutated. Forty full-length variants of ADAMTS13 exosite-3 were created and expressed. The original highly conservative gain-of-function (GoF) molecule[4] and truncated MDTCS wild-type and MDTCS 5ala variants[2] were included in this study, yielding a total of 42 ADAMTS13 variants. All the mutations were introduced into the ADAMTS13 spacer exosite-3 in full-length context and using codons most frequent in chinese hamster (*Cricetulus griseus)*.

To achieve this, a collection of synthetic 360 bp long dsDNA fragments encoding from L574 to G693 of ADAMTS13 were obtained and described below (Genewiz, Germany and Eurofins, Austria). Each fragment contained a selected mutation listed in **Supplementary Table 2** and was flanked by an *AccI* site (native in ADAMTS13 cDNA) in 5' end, and an artificially introduced *HindIII* site in 3' end (introduced by silent mutation of changing codons of Q684 and A685 from the native 5'-AGGCCT-3' DNA sequence to 5'-AAGCTT-3'). An additional longer

dsDNA synthetic fragment encoding from M509 to W688 (540 bp) and containing a native *XmaI* site flanking the 5' end region was obtained to introduce the additional mutations listed in **Supplementary Table 2**. Finally, a larger synthetic fragment of ADAMTS13 coding from F494 to C908 (1245 bp) was also obtained from the same commercial provider, already inserted into a pUC57^{Amp} cloning vector, being flanked by the native *PagI* and *Esp3I* restriction sites in 5' and 3' respectively and possessing all restriction sites mentioned above for each of the smaller fragments in the same regions (**Supplementary Table 2**). This fragment already contained the first mutation we included in our panels (F592Y). To facilitate the clone selection, an artificial *XhoI* site was introduced in this fragment by silent mutation of the codon of L621 from 5'-CTG-3' to 5'-CTC-3'. This set of ADAMTS13 cDNA fragments with desired mutations allowed for a two-step cloning process for generation of pQMCF3 expression plasmids for mutant protein production (**Supplementary Figure S1**). In the first step, the small fragment flanked by either *XmaI/HindIII* (540 bp) or *AccI/HindIII* (360 bp) is replaced in the pUC57^{Amp} vector by another fragment containing the mutations of interest, but lacking the *XhoI* site. In the next step, the larger fragment in pUC57^{Amp} flanked by *PagI/Esp3I* sites is transferred to the pQMCF3 plasmid to replace the wild-type DNA fragment (**Supplementary Figure S1**). All final constructs were sequenced before transfection.

Anti-ADAMTS13 monoclonal antibodies

Human monoclonal IgGs I-9 and II-1 were described previously[7,8]. Their V_H and V_L coding genes were inserted into a pVin-hIgG1 vector (Icosagen Cell Factory, OÜ) containing constant regions of human IgG1 heavy and kappa light chain. They were expressed in CHO cells as described below, and purified[8]. Murine antibodies 3H9 (anti-metalloprotease), and biotinylated 19H4 (anti-TSP8) and 17G2 (anti-CUB1) were also previously described[9,10]. Anti-V5 conjugated with horseradish peroxidase was obtained from Invitrogen® (Catalog # R96125).

Expression of the ADAMTS13 mutants and anti-ADAMTS13 monoclonal antibodies

A CHO-based cell-line specifically modified for QMCF technology (CHOEBNALT85 clone 1E9, European Patent EP1851319B1, Icosagen Cell factory OÜ, Estonia) was cultured in suspension in BalanCD CHO Transfectory Medium (Irvine Scientific, USA), supplemented with Glutamax 6mM and Penicillin-Streptomycin 1%, at 37°C. Cells were transfected with each of the

sequenced pQMCF3 ADAMTS13 mutant constructs as described[11]. An additional culture with a mock transfection was used for control and cultured in the same conditions. Proteins were transiently expressed with a temperature shift to 30°C at 72h-96h post-transfection (cell densities > $3x10^6$/mL). Feed 4 (Irvine Scientific, USA) was added every 2 days according to manufacturers' instructions starting at day 3 until day 11 post-transfection, and cell viability was maintained ≥90%. Supernatants were collected between days 10-14 post transfection, or earlier if viability became lower. Cell mass and cell debris was cleared by centrifugation. PMSF (Serva, Germany) was added to all supernatants (final concentration 0.5 mM). ADAMTS13 protein expression was confirmed by Western Blot using a mouse anti-HisTag antibody (GenScript, USA) and a goat anti-mouse-IgG-HRP (GenScript, USA), or an anti-V5-HRP antibody (Invitrogen) directly stained in PVDF membranes with a TMB III solution *(data not shown)*. Human monoclonal IgGs I-9 and II-1[7,8] were expressed as hIgG1/kappa antibodies from pVin-hIgG1 vector (Icosagen Cell Factory OÜ, Estonia) in a similar manner.

Quantitation of ADAMTS13 in the supernatants

The full-length mutants were quantified in supernatants employing an in-house-developed ELISA assay with modifications[10]. Briefly, maxisorp ELISA plates (Nunc®) were coated with 3H9 mouse antibody overnight 4 ^oC (5 ug/mL). They were then aspirated and blocked for 2 hours with BSA 2%-Tween20 0.05% in PBS pH 7.6 (200 uL/well, room temperature). Next, they were washed 6x with PBS-Tween 20 0.1% in a plate washer (Skan Washer 400, Molecular Devices) and normal human plasma (NHP) – considered to contain 1 ug/mL ADAMTS13[12] – was used as a calibrator, serially diluted 1/2 in PBS-BSA 1%-Tween 20 0.05%, starting at a dilution of 1/2 (dilution range: 1/2 – 1/256). The supernatants were also serially diluted in the same fashion (range: 1/4 – 1/64 for full length supernatants and control supernatant; 1/10 – 1/1600 for MDTCS supernatants). All samples including calibrator were diluted in separate tubes and 100 uL of each dilution were transferred to the plates. Samples were incubated for 1 hour at 37 ^oC. Afterwards, the plates were washed 6x, and previously described biotinylated antibodies 19H4 (anti-TSP_8) and 17G2 (anti-CUB_1)[13] were incubated in all samples at 1.5 ug/mL (100 uL/well) for 1h at 37 ^oC. After washing, 100 uL/well of 1:10000 streptavidin-HRP (Invitrogen) were added, and incubated at room temperature for 1 hour. Finally, the plates were washed

again, and developed using a TMB solution (100 uL/well) for 3 minutes, with reaction being stopped with H_2SO_4 1 M (50 uL/well). The plates were then read for OD at 450 nm (reference 540 nm) in a plate reader (SpectraMax Plus^{384}, Molecular Devices). The supernatants of the truncated ADAMTS13 variants were quantified in a modified manner because these variants lack the C-terminal domains which constitute the epitopes of the 19H4 and 17G2 antibodies. For these, a previously quantified full-length ADAMTS13 wild-type supernatant was used as a calibrator, containing a variant with the same C-terminal V5-His tag as the truncated variants. The truncated variants supernatants were serially diluted as stated above. For detection, an anti-V5-HRP antibody was used (dilution: 1:2500; 100 uL/well), and incubated at room temperature for 1 hour. The plates were washed again, and developed using a TMB solution (100 uL/well) for 30 minutes, with reaction being stopped as described above. The plates were then read as stated above. The molecular mass difference was taken into account, with the full-length ADAMTS13 wild-type variant considered to have 190 KDa and the MDTCS variants 75 KDa, as evaluated by SDS-PAGE western-blot. For both methods, sigmoidal calibration curves were obtained, and fitted with a 4-parameter fit curve (GraphPad Prism 5.0). Interpolation was made using the OD values within the linear area of the curve with 95% confidence interval.

ELISA assay to assess the patients' samples reactivity towards the ADAMTS13 variants

ELISA Maxisorp plates (Nunc®) were coated with antibody 3H9 at 1 ug/mL to capture ADAMTS13 from cell culture medium[14]. The plates were then blocked with a solution of BSA 2%-Tween20 0.05%-saccharose 2% in PBS, and dried overnight at 30 ^{o}C in a heater in the presence of desiccant (silica-gel). All plates were stored at 4 ^{o}C under vacuum in sealed aluminum foil bags with desiccant (Minipax®, Multisorb Technologies Inc) until use.

The proper dilution for each patient sample was determined experimentally, by incubating a serial dilution of the patients' samples against the full-length wild-type ADAMTS13 variant, in the same conditions of the final assay. Dilutions ranged from 30x-1200x, according to need. A I-9 or II-1 monoclonal antibody dilution curve was included against the same variant. The best patient dilution was considered as the one having the highest signal below the saturation upper plateau area of the I-9 or II-1 curve, while having the lowest possible background. A 'target OD' of 1.6 was set, and the patients' best dilutions are shown in

Supplementary Figure S2. Each patient sample was then tested for reactivity (i.e. binding of autoantibodies) against the variants described above. Each sample was assessed against 200 ng of each ADAMTS13 full-length variant or to equal molar quantities of the MDTCS variants, in duplicate. ADAMTS13 variants' supernatants were diluted in PBS-BSA1%-Tween20 0.05% buffer and captured by 3H9 for 1h at 37 ^{o}C. A supernatant from mock-transfection of CHO cells was included for background assessment. The patient samples were then diluted in the same buffer and incubated 1h at 37 ^{o}C. Finally, a pool of monoclonal antibodies against human-IgG1, IgG2, IgG3 and IgG4, each conjugated with HRP (Sanquin, The Netherlands) was used for detection (dilution of 1:10000 each, 1h, room temperature). A TMB solution was used for signal development for 10 minutes and reactions stopped with H_2SO_4 1 M. Plates ODs were read at 450 nm (540 nm as reference) (SpectraMax Plus^{384}, Molecular Devices). In each plate, a monoclonal antibody II-1 dilution curve against the full-length wild-type ADAMTS13 was fitted with a non-linear regression curve 4-parameter fit (Log Agonist VS Response Non-Linear (Four Parameters)) (GraphPad Prism 5.0). Reactivity of the patient sample to each of the variants was converted into II-1 equivalent units by direct interpolation of the II-1 curve. The reactivity of the wild-type was considered 100% for each patient. An example of the calculations made is given in **Supplementary Figure S3**.

Molecular modeling of ADAMTS13 Spacer Domain Exosite-3 mutants

The ADAMTS13 Spacer domain crystal structure was obtained from Protein Data Bank (the deposited structure spans the Disintegrin-like domain, thrombospondin type-1 repeat, cysteine-rich and spacer domains, Protein Data Bank ID: 3GHM)[15] Spacer domain mutations (RARAA, AAAAA, GoF (KYKFF), RNRNN, RLRLL) were introduced with the mutagenesis module of PyMOL 1.8.2.1 (The PyMOL Molecular Graphics System, Version 1.8.2.1 Schrödinger, LLC). Wild-type and mutant spacer domain structures were prepared for molecular dynamics (MD) simulations assigning the AMBER force field FF14SB[16] in AMBER 16[17] package. The simulation systems were solvated by the TIP3P[18] water model within a 10 Å radius of the molecular surface of the structures. Following the addition of the solvent, the total charge of the systems was neutralized by Na^+ and Cl^- counter ions which were successively added by replacement of water. Steepest descent energy minimization was initiated through 2000 steps which was followed by

2000 steps of conjugate gradient algorithm to adjust positions of solvent molecules with fixed solute molecule positions. Hence, the energy of the whole system was minimized without any position-restrained molecules. Following the minimization steps, the systems were progressively heated from 0 to 300 K in a position-restrained MD simulation for 100 ps with a collision frequency of 1 ps^{-1} on Langevin dynamics. During this heating step, the solute molecules were restrained with a weak force constant (10 kcal/mol). Hereafter, the systems were equilibrated for 400 ps at a constant 300 K temperature with the same position-restrain parameters as in the previous step. Following these position-restrained phases, a free-production phase was started with constant temperature at 300 K and 1 bar pressure for 50 ns simulation time. The SHAKE algorithm[19] was applied at time steps of 2 fs in order to maintain the correct bond geometry throughout the MD simulation. The Particle-mesh Ewald (PME)[20] method was used to calculate the electrostatic interactions and non-bonded interactions were computed at 10 Å cutoff. An additional accelerated MD (aMD) simulation[21] of 250 ns was carried to investigate any possible conformational change in ADAMTS13 spacer domain. A total of 300 ns MD simulation trajectories for each spacer variant including WT were investigated by cpptraj.[22] End-point snapshots from each trajectory were extracted to calculate the changes on electrostatic potential molecular surface between each variant by the APBS plugin[23] in PyMOL.

Testing the activity of selected variants in a VWF multimer assay

Seakem® HGT(P) Agarose (Lonza) was melted in a water bath at 300 ^{o}C and used to cast gels (resolving gel 1.8% *m/v*; stacking gel 0.75% *m/v*). The resolving gel was casted with a buffer with the following composition: Tris-base 0.2 M, glycine 0.1 M and SDS 0.4% *m/v*, pH=9.0. The stacking gel was casted with a buffer with the following composition: Tris-base 0.07 M, EDTA 0.004 M and SDS 0.4% *m/v*, pH=6.7. An ADAMTS13 activating buffer was used to incubate supernatants of ADAMTS13 prior to reaction initiation (buffer composition: 25 mM $CaCl_2$, Bis-Tris 20 mM, Tris-HCl 20 mM, HEPES 20 mM, Tween20 0.005%, pH = 7.5, and 2% Bovine Serum Albumin fraction V (Merck)). ADAMTS13 (200 ng) was incubated with the activating buffer

(equal volumes) for 30 mins at 37 ^{o}C. In parallel, recombinant VWF supernatant produced in HEK293 cells (stock concentration = 336 nM) was incubated with 3 M urea for 30 min at 37^{o}C (VWF concentration: 80 nM). The denatured recombinant VWF multimers were then added directly to the activated ADAMTS13 in equal volumes, and the reaction was sampled at time-points 0 mins, 30 mins and 24 h, being quenched with 4x loading buffer (composition: urea 9.6 M, 4% SDS *m/v*, Tris-base 0.035 M, EDTA 25 mM, Bromophenol blue 7.5 µM, no pH adjustment). The final concentrations of each component in the reaction were: ADAMTS13 1.9 nM, VWF 40 nM, urea 1.5 M, BSA 0.5%, all other buffer components diluted 4x. The gels were run at 100 V, 35 mA, 12.5W (with constant voltage) for 1h55mins in a Tris-Glycine Buffer with SDS (0.1 M Tris-base, 0.15 M glycine, 4% SDS *m/v*). Finally, each gel was transferred to a PVDF membrane by capillary transfer overnight (PBS used for the transfer), and the detection of the VWF multimers was done with a rabbit anti-hVWF-HRP polyclonal antibody diluted 1:2000 (Dako, P0226). VWF multimers were visualized employing DAB stain (Vector Labs) directly on the membrane.

Supplementary References

1. Luken BM, Turenhout EAM, P Kaijen PH, et al. Amino acid regions 572–579 and 657–666 of the spacer domain of ADAMTS13 provide a common antigenic core required for binding of antibodies in patients with acquired TTP Blood Coagulation, Fibrinolysis and Cellular Haemostasis. *Thromb. Haemost.* 2006;96:295–301.
2. Pos W, Sorvillo N, Fijnheer R, et al. Residues arg568 and phe592 contribute to an antigenic surface for anti-adamts13 antibodies in the spacer domain. *Haematologica*. 2011;96(11):1670–1677.
3. Silla T, Haal I, Geimanen J, et al. Episomal Maintenance of Plasmids with Hybrid Origins in Mouse Cells. *J. Virol.* 2005;79(24):15277–15288.
4. Jian C, Xiao J, Gong L, et al. Gain-of-function ADAMTS13 variants that are resistant to autoantibodies against ADAMTS13 in patients with acquired thrombotic thrombocytopenic purpura. *Blood*. 2012;119(16):3836–3843.
5. Jin S-Y, Skipwith CG, Zheng XL. Amino acid residues Arg659, Arg660, and Tyr661 in the spacer domain of ADAMTS13 are critical for cleavage of von Willebrand factor. *Blood*. 2010;115(11):2300–2310.
6. Pos W, Crawley JTB, Fijnheer R, et al. An autoantibody epitope comprising residues R660, Y661,

and Y665 in the ADAMTS13 spacer domain identifies a binding site for the A2 domain of VWF. *Blood*. 2010;115:1640–1649.

7. Pos W, Luken BM, Kremer Hovinga JA, et al. VH1-69 germline encoded antibodies directed towards ADAMTS13 in patients with acquired thrombotic thrombocytopenic purpura. *J. Thromb. Haemost.* 2009;7(3):421–428.

8. Luken BM, Kaijen PHP, Turenhout EAM, et al. Multiple B-cell clones producing antibodies directed to the spacer and disintegrin/thrombospondin type-1 repeat 1 (TSP1) of ADAMTS13 in a patient with acquired thrombotic thrombocytopenic purpura. *J. Thromb. Haemost.* 2006;4:2355–2364.

9. Feys HB, Roodt J, Vandeputte N, et al. Thrombotic thrombocytopenic purpura directly linked with ADAMTS13 inhibition in the baboon (Papio ursinus). *Blood*. 2010;116(12):2005–2010.

10. Alwan F, Vendramin C, Vanhoorelbeke K, et al. Presenting ADAMTS13 antibody and antigen levels predict prognosis in immune-mediated thrombotic thrombocytopenic purpura. *Blood*. 2017;130(4):466–471.

11. Karro K, Männik T, Männik A, Ustav M. DNA Transfer into Animal Cells Using Stearylated CPP Based Transfection Reagent. *Cell-penetrating Pept. Methods Protoc.* 2015;435–445.

12. Feys HB, Liu F, Dong N, et al. ADAMTS-13 plasma level determination uncovers antigen absence in acquired thrombotic thrombocytopenic purpura and ethnic differences. *J. Thromb. Haemost.* 2006;4:955–962.

13. Deforche L, Roose E, Vandenbulcke A, et al. Linker regions and flexibility around the metalloprotease domain account for conformational activation of ADAMTS-13. *J. Thromb. Haemost.* 2015;13:2063–2075.

14. Roose E, Vidarsson G, Kangro K, et al. Anti-ADAMTS13 Autoantibodies against Cryptic Epitopes in Immune-Mediated Thrombotic Thrombocytopenic Purpura. *Thromb. Haemost.* 2018;118(10):1729–1742.

15. Akiyama M, Takeda S, Kokame K, et al. Crystal structures of the noncatalytic domains of ADAMTS13 reveal multiple discontinuous exosites for von Willebrand factor. *Proc. Natl. Acad. Sci.* 2009;106(46):19274–19279.

16. Maier JA, Martinez C, Kasavajhala K, et al. ff14SB: Improving the Accuracy of Protein Side Chain and Backbone Parameters from ff99SB. *J. Chem. Theory Comput.* 2015;11(8):3696–3713.

17. Case DA, Berryman JT, Betz RM, Cerutti DS, Cheatham I. AMBER 2017. 2017;

18. Jorgensen WL, Chandrasekhar J, Madura JD, Impey RW, Klein ML. Comparison of simple potential functions for simulating liquid water. *J. Chem. Phys.* 1983;79(2):926–935.

19. Ryckaert JP, Ciccotti G, Berendsen HJC. Numerical integration of the cartesian equations of motion of a system with constraints: molecular dynamics of n-alkanes. *J. Comput. Phys.* 1977;23(3):327–341.

20. Darden T, York D, Pedersen L. Particle mesh Ewald: An $N \cdot \log(N)$ method for Ewald sums in large systems. *J. Chem. Phys.* 1993;98(12):10089–10092.

21. Pierce LCT, Salomon-Ferrer R, Augusto C, et al. Routine access to millsecond timescale evenrs with accelerated molecular dynamics. *J. Chem. Theory Comput.* 2012;Accepted.

22. Roe DR, Cheatham III TE. PTRAJ and CPPTRAJ: software for processing and analysis of molecular dynamics trajectory data. *J Chem Theory Com*. 2013;9(7):3084–3095.

23. Jurrus E, Engel D, Star K, et al. Improvements to the APBS biomolecular solvation software suite. 2018;27:112–128.

24. Klaus C, Plaimauer B, Studt JD, et al. Epitope mapping of ADAMTS13 autoantibodies in acquired thrombotic thrombocytopenic purpura. *Blood*. 2004;103(12):4514–4519.

25. Luken BM, Turenhout EAM, Hulstein JJJ, et al. The spacer domain of ADAMTS13 contains a major binding site for antibodies in patients with thrombotic thrombocytopenic purpura. *Thromb. Haemost.* 2005;93:267–74.

26. Long Zheng X, Wu HM, Shang D, et al. Multiple domains of ADAMTS13 are targeted by autoantibodies against ADAMTS13 in patients with acquired idiopathic thrombotic thrombocytopenic purpura. *Haematologica*. 2010;95(9):1555–1562.

27. Yamaguchi Y, Moriki T, Igari A, et al. Epitope analysis of autoantibodies to ADAMTS13 in patients with acquired thrombotic thrombocytopenic purpura. *Thromb. Res.* 2011;128:169–173.

28. Grillberger R, Casina VC, Turecek PL, et al. Anti-ADAMTS13 IgG autoantibodies present in healthy individuals share linear epitopes with those in patients with thrombotic thrombocytopenic purpura. *Haematologica*. 2014;99:e58–e60.

29. Casina VC, Hu W, Mao J-H, et al. High-resolution epitope mapping by HX MS reveals the pathogenic mechanism and a possible therapy for autoimmune TTP syndrome. *Proc. Natl. Acad. Sci.* 2015;112(31):9620–9625.

30. Thomas MR, de Groot R, Scully MA, Crawley JTB. Pathogenicity of Anti-ADAMTS13 Autoantibodies in Acquired Thrombotic Thrombocytopenic Purpura. *EBioMedicine*. 2015;2:942–952.

31. Ostertag EM, Kacir S, Thiboutot M, et al. ADAMTS13 autoantibodies cloned from patients with acquired thrombotic thrombocytopenic purpura: 1. Structural and functional characterization in vitro. *Transfusion*. 2016;56(7):1763–1774.

Supplementary Table 1 – Summary of previous epitope mapping studies of acquired TTP patients' autoantibody repertoires against ADAMTS13.

Study author and year	Number of patients in study	Patients with autoantibodies against metalloprotease/disintegrin/TSP1 domains		Patients with autoantibodies towards cys-rich/spacer domain (exosite-3 and other unknown epitopes)		Patients with autoantibodies against C-terminal domains (TSP2-8 and/or CUBs)	
		Total	Percentage	Total	Percentage	Total	Percentage
Klaus et al, 2004[24]	25	14	56%	25	100%	17	68%
Luken et al, 2005[25]	6	0	0%	6	100%	1	16.7%
Luken et al, 2006[1]	6	N.A.	N.A.	6	100%	N.A.	N.A.
Long Zheng et al, 2010[26] **	67	8	11.9%	65	97%	32	47.8%
Pos et al, 2010[6]	5	0	0%	5	100%	0	0%
Pos et al, 2011[2]	48	N.A.	N.A.	48	100%	21	43.8%
Yamaguchi et al, 2011[27] *	13	5	38.5%	8	61.5%	10	76.9%
Jian et al, 2012[4]	12	N.A.	N.A.	12	100%	N.A.	N.A.
Grillberger et al, 2014[28]	3	2	66.6%	2	66.6%	3	100%
Casina et al, 2015[29]	23	N.A.	N.A.	20	87%	N.A.	N.A.
Thomas et al, 2015[30] **	92	0	0%	89	96.7%	54	58,7%
Ostertag et al, 2016[31]	4	1	25%	3	75%	1	25%
Total	304	30 (of 215 patients tested)	~ 14.0%	289 (of 304 patients tested)	~ 95.1%	139 (of 263 patients assessed)	52.9%

* Yamaguchi's study employed a phage display technique that targeted only linear peptides. If one excludes this study owing to the methodology, the final numbers become: 282/296 = ~95,3% and 129/254 = 50.8%

** These two studies reported very similar numbers of patients having autoantibodies against the N-terminal domains only: Long Zheng *et al.* reported that 29/67 patients (43%) had autoantibodies against the cys-rich-spacer domains only, while Thomas *et al.* reported that 38/92 patients (41%) had autoantibodies exclusively recognizing the spacer domain.

N.A. = Not Assessed

Supplementary Table 2: DNA oligonucleotide fragments and spacer exosite-3 mutations carried by each fragment.

Bold enzymes indicate the native restriction sites in the *ADAMTS13* human gene. All others were artificially introduced for cloning purposes without mutation of the aminoacid residues.

Fragments	Length	Relevant restriction sites (in order from 5'→3')	Mutation panel (mutations in each panel summarized)	Variant Designation	Final Exosite-3 residues summary
----------	Full-length	----------	Wild Type ADAMTS13	WT	R F R Y Y (original exosite-3)
----------	MDTCS	----------	Truncated ADAMTS13 variant (no C-terminal TSP2-8 and CUB1-2 domains)	MDTCS WT	R F R Y Y (original exosite-3)
----------	MDTCS	----------	Truncated ADAMTS13 variant (no C-terminal TSP2-8 and CUB1-2 domains)	MDTCS AAAAA	A A A A A
Large	1245 bp	***PagI; XmaI; AccI;*** *XhoI; HindIII;* ***Esp3I*** Coding aa residues in ADAMTS13: F494-C908	Conservative Panel (Y ↔ F)	Mut 1.1	R Y R Y Y
Small	360 bp	***AccI;*** *HindIII* Coding aa residues in ADAMTS13: L574-G673		Mut 2.1	R F R F Y
				Mut 3.1	R F R Y F
				Mut 4.1	R Y R F Y
				Mut 5.1	R Y R Y F
				Mut 6.1	R F R F F
				Mut 7.1	R Y R F F
			Semi-Conservative Panel (Y or F → L)	Mut 8.1	R L R Y Y
				Mut 9.1	R F R L Y
				Mut 10.1	R F R Y L
				Mut 11.1	R L R L Y
				Mut 12.1	R L R Y L
				Mut 13.1	R F R L L
				Mut 14.1	R L R L L
			Non-Conservative Panel (Y or F → N)	Mut 15.6	R N R Y Y
				Mut 16.13	R F R N Y
				Mut 17.1	R F R Y N
				Mut 18.1	R N R N Y
				Mut 19.1	R N R Y N
				Mut 20.1	R F R N N
				Mut 21.1	R N R N N
			Main alanine panel (Y or F → A)	Mut 22.2	R A R A A
				Mut 23.1	R A R Y Y
				Mut 24.1	R F R A Y
				Mut 25.1	R F R Y A
				Mut 26.1	R A R A Y
				Mut 27.1	R A R Y A
				Mut 28.1	R F R A A

	540 bp	***Xmal;*** *AccI; HindIII* Coding aa residues in ADAMTS13: M509-W688	Classic 5ala mutant	Mut 29.1	A A A A A
			Gain-of Function, Jian et al, 2012	Mut 30.1	K Y K F F
			Arginine mutation panel (R → A, ± Y or F →A)	Mut 31.2	A F R Y Y
				Mut 32.2	R F A Y Y
				Mut 33.1	A F A Y Y
			Arginine mutation panel (R → A, ± Y or F →A)	Mut 34.1	A A R A A
				Mut 35.1	R A A A A
			Alanine/Lysine Hybrid panel (R → A or K, + Y or F → A)	Mut 36.2	A A K A A
				Mut 37.2	K A A A A
				Mut 38.1	K A K A A
				Mut 39.1	K A R A A

Supplementary Figures Legends

Supplementary Figure S1. Cloning steps for full-length ADAMTS13 mutants created for this study.
Synthetic oligonucleotides (360bp spanning from L574 to G693 and 540 bp spanning from M509 to W688) containing the desired mutations were ordered. Mutant 1 was ordered embedded in a larger oligonucleotide fragment of *ADAMTS13* spanning from the F494 to C908 (1245 bp), and inserted into the pUC57^{Amp} vector.

The *ADAMTS13* wild-type native sequence does not possess the enzyme sites in red. These were artificially introduced without creating additional residue mutations. In pUC57_mut1 possesses native *PagI, XmaI* and *Esp3I* sites, and artificial *AccI*, *XhoI, and HindIII* sites. The other small fragments are flanked either by *AccI/HindIII* (360 bp), or by *XmaI/HindIII* (540 bp), and none contain the artificial *XhoI* site of mutant 1. The mutant 1 fragment in pUC57 is replaced by means of *AccI/HindIII*, or *XmaI/HindIII* restriction, creating several large fragments carrying the different mutations. Then, these large ADAMTS13 fragments with the desired mutations are excised by *PagI/Esp3I* digestion and used to replace the native gene sequence of ADAMTS13-V5-His in pQMCF3. The mutants are distinguishable from the wild-type variant through *HindIII* digestion, and from mutant 1 through *XhoI* digestion, but are not distinguishable from each other on agarose gel electrophoresis. Each plasmid is sequenced to confirm the correct mutations are inserted.

Supplementary Figure S2. Patient dilution curves compared to I-9 or II-1 dilution curves (treated data without background). Monoclonal antibodies I-9 or II-1 were diluted and assessed against 200 ng of captured full-length ADAMTS13 wild-type. A 'target OD' was arbitrarily defined as the best possible wild-type reactivity value for all patients. However, patients' reactivities may be highly variable. Thus, a window of 'acceptable' OD values was arbitrarily set between 1.0 and 1.7. By default, all mutants were expected to have either as high or lower reactivity towards autoantibodies compared to the wild-type. Patients' serial dilutions were made with the goal of assessing the highest patient dilution giving the highest signal below the saturation zone of the I-9 and II-1 curves, simultaneously having the lowest background possible. Some patients required lower dilutions (e.g. patients TTP-007, -012 and -017), while others required higher dilutions (patients TTP-008, -052 and -085). Three patients inherently have low signals even at dilutions of 30x.

Supplementary Figure S3. Example of Calculations to build Heat-map of Figure 2.

All plates were arranged in the same manner, with as many variants inserted as possible. One patient was assessed per plate. In each plate, a dilution curve of antibody II-1 against the full-length wild-type is inserted. Each mutant variant is incubated (200 ng of each for full-length, same molar quantity for MDTCS variants, 1.05 nmol). For antibody II-1 the concentration range of the dilution curve spans 250 ng/mL to 0.1 ng/mL. Data is collected and is first corrected with the respective background signals (subtracted where appropriate). The II-1 dilution curve is used for interpolation of each well's signal to convert into II-1 equivalent units (ng/mL). The dilution factor is applied. Next, the ratio of each well is calculated as a measure of relative reactivity (average WT full-length reactivity is 100%). All well's values are plotted as shown, for each patient and average values were used to build the heat map presented in Figure 2.

Supplementary Figure S4. Example of Calibration Curve for ADAMTS13 variants' activity calculations.

Full-length wild-type supernatant was diluted for the concentrations shown and put to react with 0.4 µmol of FRETS-VWF73 substrate. A typical calibration curve is shown. A 4-parameter fit was used for data interpolation, with 10000 iterations and 95% confidence interval in Graphpad Prism 5.0.

Supplementary Figure S5. WT-ADAMTS13 Spacer domain epitope intramolecular interactions.

Arg568 and Tyr665 form a hydrogen bond (yellow dashes). Arg568 also forms cation-pi interactions with both Tyr661 and Tyr665 (black dashes). Arg660 also forms a cation-pi interaction with Tyr661 (black dashes).

Supplementary Figure S6. Models of 3D structure and solvent accessible surface area size of RFRYY epitope on WT- and other-ADAMTS13 variants.

A. Wild-type (RFRYY). B. Triple-alanine mutant variant (RARAA). C. 5x Alanine mutant variant (AAAAA). D. Classic Gain-of-Function (KYKFF). E. Triple-asparagine non-conservative mutant variant (RNRNN) F. Semi-conservative mutant (RLRLL)

Supplementary Figure S7. Characterization of wild-type and classic gain-of-function ADAMTS13 full-length molecules expressed in CHO cells and HEK293 cells.

A. Western blot of CHO and HEK293 ADAMTS13 wild-type and classic GoF full-length molecules (supernatants directly loaded). Proteins were blotted with a-V5-HRP antibody. Lanes: 1 – CHO wild-type; 2 – CHO GoF; 3 – HEK293 wild-type; 4 – HEK293 GoF. B. FRETS-VWF73 assay curves for supernatants from CHO and HEK293 ADAMTS13 wild-type and GoF. The HEK293 supernatants were diluted to have the same concentrations employed with the CHO wild-type molecule (range: 0.025-0.4 ug/mL) and curves were fitted with a 4 parameter curve fit (Graphpad Prism 5.0). The classic GoF from CHO cells was only assessed at a concentration of 0.2 ug/mL. The same gene of interest was expressed both in CHO and in HEK293 cells. C. VWF multimer assay with wild-type and GoF ADAMTS13 variants expressed in HEK293 cells. D. Binding of patient samples to each of the CHO and HEK293 ADAMTS13 molecules in ELISA (heat map). The normalization and interpolation was made with each respective wild-type signal. The GoF molecules show the same reactivity level compared to their respective wild-type molecules. Data of 12 patients are presented. E. OD signals obtained for each molecule screened with the 12 patients shown in the heat map. The OD signal was very similar.

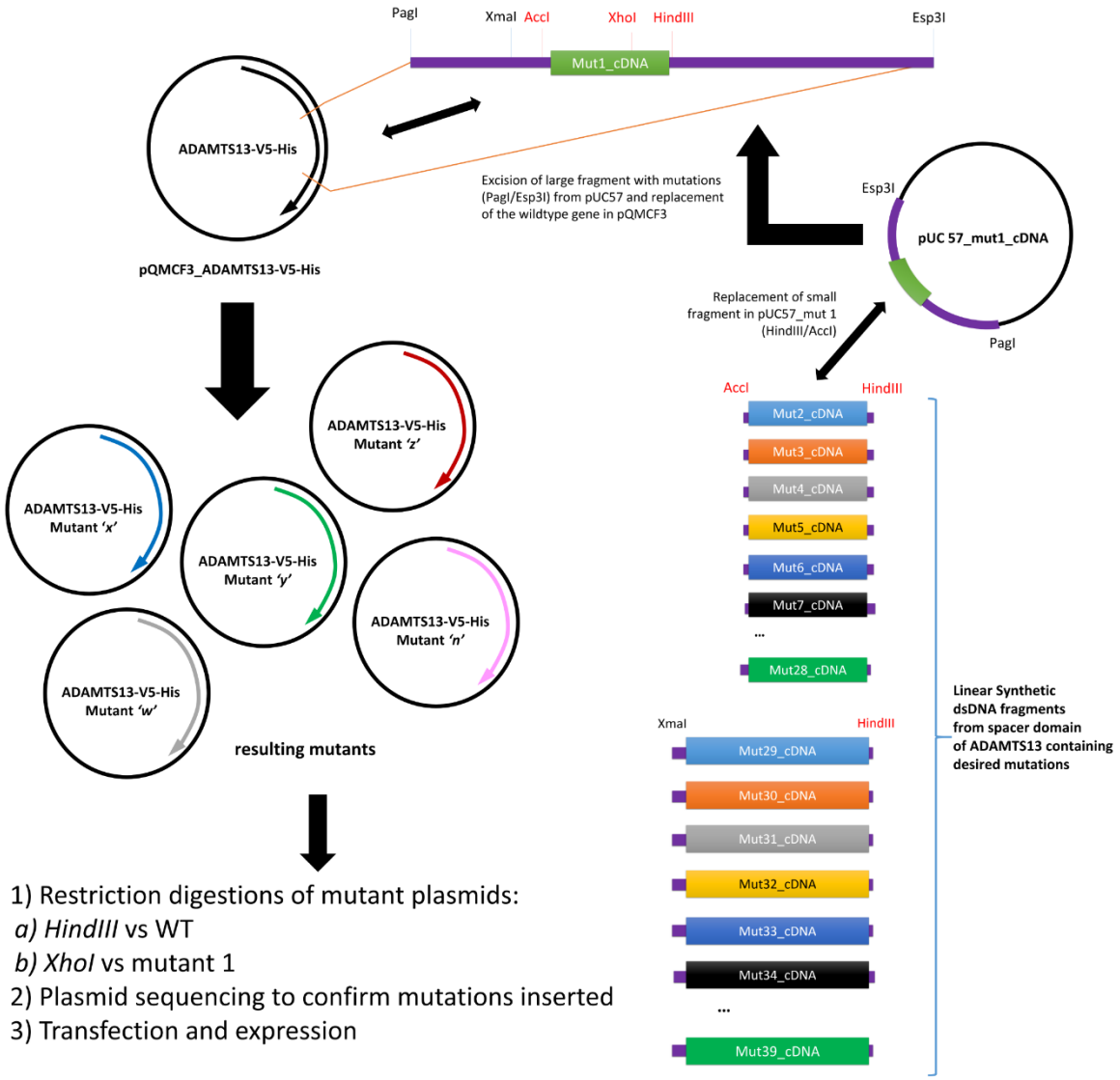

Supplementary Figure S1.

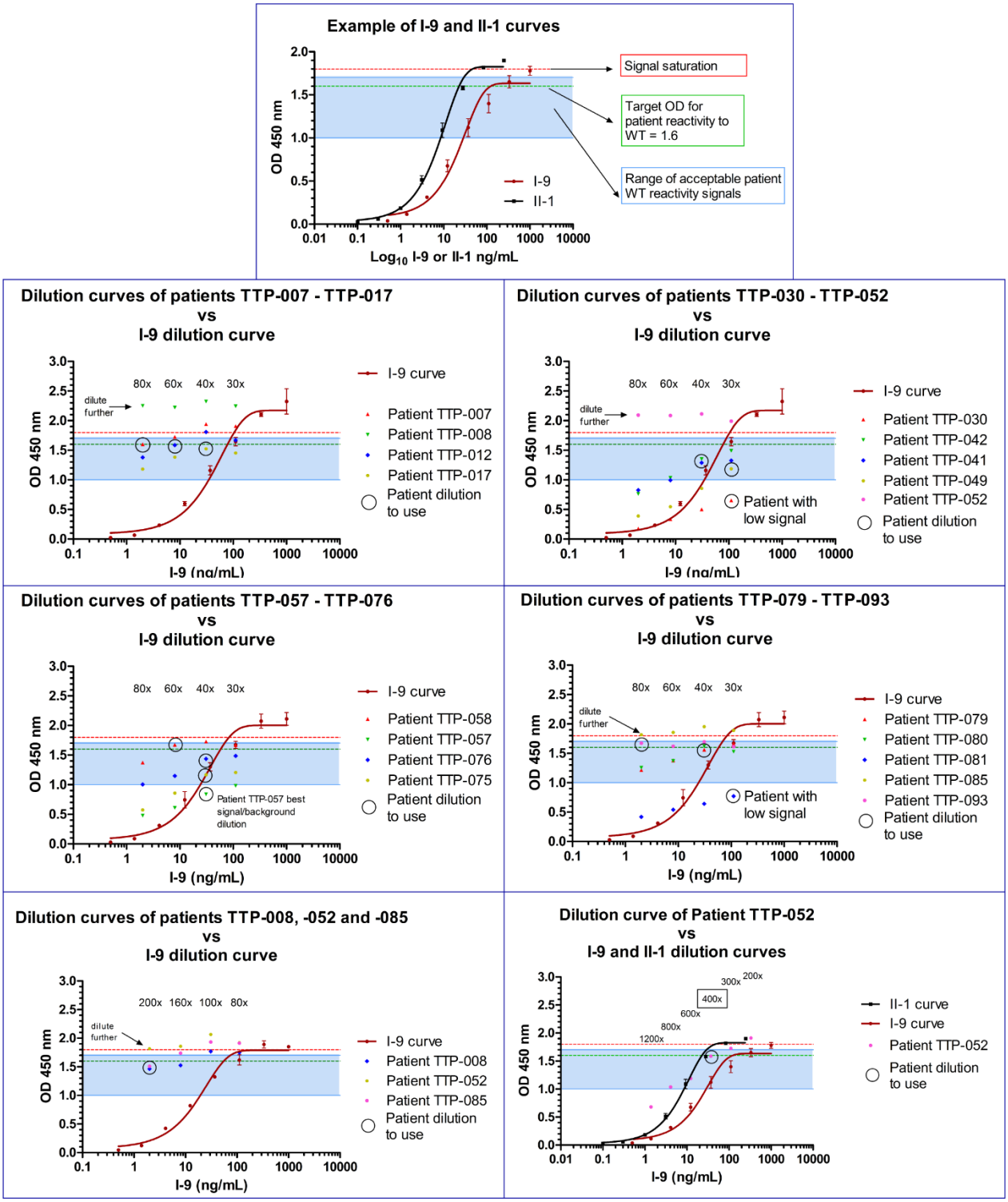

Supplementary Figure S2

Example of Calculations

	1	2	3	4	5	6	7	8	9	10	11	12
A	NP CHO vs 250 ng/mL	250	250	WT	WT	mut 7	mut 7	mut 15	mut 15	mut 23	mut 23	MDTCS WT
B	NP CHO vs 250 ng/mL	83,3	83,3	WT	WT	mut 8	mut 8	mut 16	mut 16	mut 24	mut 24	MDTCS WT
C	WT CHO vs 9,3 ng/mL	27,8	27,8	mut 1	mut 1	mut 9	mut 9	mut 17	mut 17	mut 25	mut 25	MDTCS 5ala
D	WT CHO vs 9,3 ng/mL	9,3	9,3	mut 2	mut 2	mut 10	mut 10	mut 18	mut 18	mut 26	mut 26	MDTCS 5 ala
E	NP CHO vs 9,3 ng/mL	3,1	3,1	mut 3	mut 3	mut 11	mut 11	mut 19	mut 19	mut 27	mut 27	NP
F	NP CHO vs 9,3 ng/mL	1	1	mut 4	mut 4	mut 12	mut 12	mut 20	mut 20	mut 28	mut 28	NP
G	Blanks + Sec	0,3	0,3	mut 5	mut 5	mut 13	mut 13	mut 21	mut 21	mut 29	mut 29	NP
H	Blanks + Sec	0,1	0,1	mut 6	mut 6	mut 14	mut 14	mut 22	mut 22	mut 30	mut 30	NP

Data collection

	1	2	3	4	5	6	7	8	9	10	11	12
A	-0,003	2,339	2,373	1,689	1,637	1,515	1,599	1,333	1,221	1,203	1,249	1,484
B	0,003	2,405	2,417	1,789	1,704	1,623	1,608	1,457	1,433	1,473	1,439	1,577
C	1,998	2,313	2,238	1,637	1,578	1,611	1,625	1,650	1,625	1,560	1,617	0,142
D	1,839	2,007	2,038	1,713	1,709	1,671	1,672	0,722	0,744	0,973	0,869	0,155
E	-0,001	1,351	1,358	1,724	1,651	1,388	1,447	0,840	0,798	1,132	1,124	-0,001
F	-0,002	0,588	0,604	1,608	1,578	1,534	1,536	1,201	1,291	1,200	1,191	-0,009
G	0,002	0,207	0,212	1,566	1,646	1,474	1,531	0,349	0,372	0,336	0,322	-0,007
H	-0,002	0,068	0,070	1,644	1,547	1,276	1,327	0,726	0,668	1,277	1,246	0,016

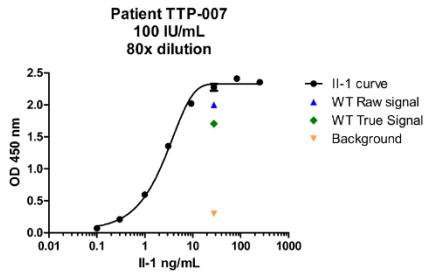

Interpolation of values in each well

1) Patients' signal in wells converted to II-1 equivalents (ng/mL) and multiplied by Dilution factor
2) Full-length wild-type average is set at 100%;
3) Calculation of ratio 'variant'/'WT average' (values of equivalents) for each well;
4) Plot patient reactivity data

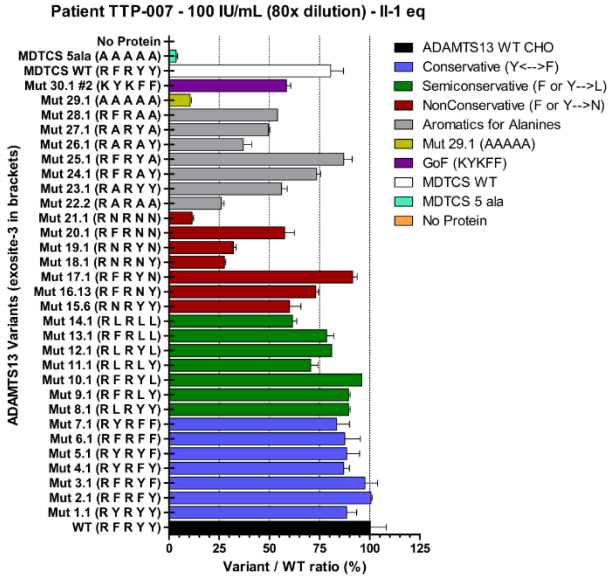

Heat-Map (Figure 2)

Supplementary Figure S3.

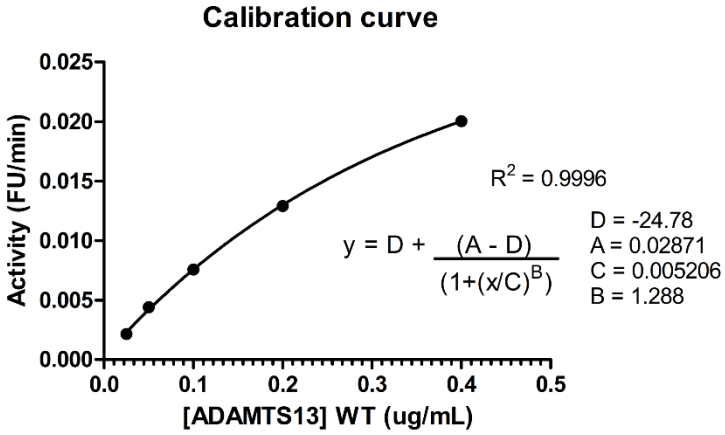

Supplementary Figure S4.

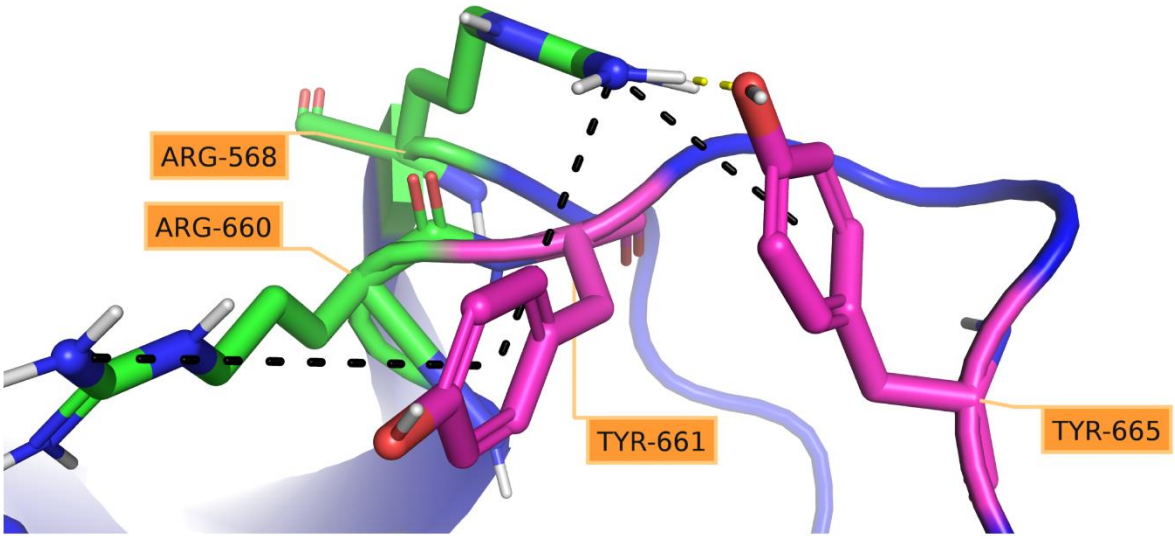

Supplementary Figure S5.

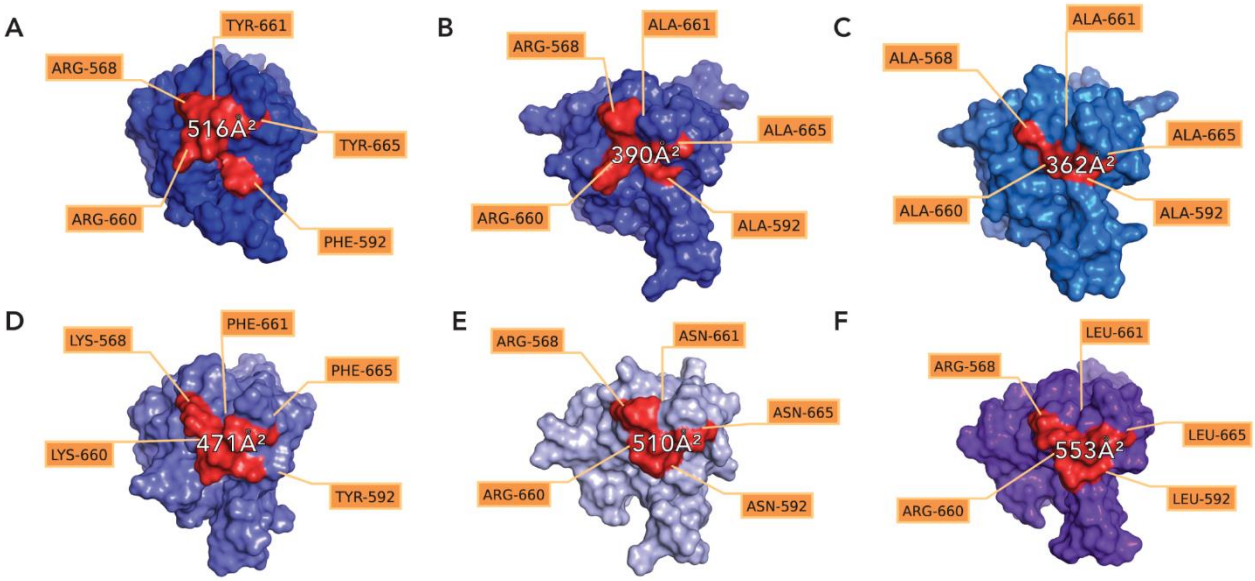

Supplementary Figure S6.

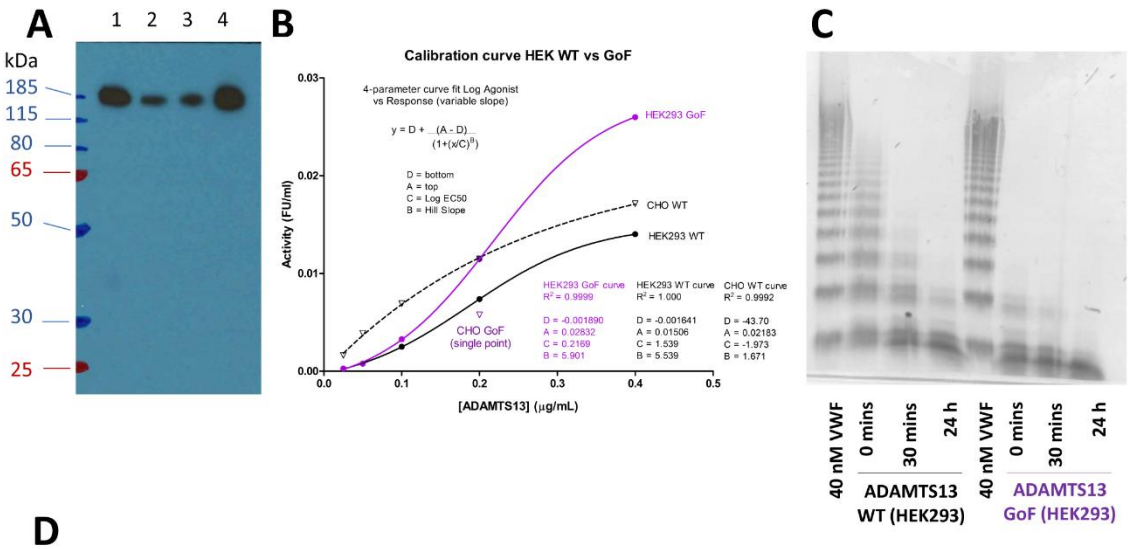

D

Mutant Variants (exosite-3 residues)		Patients tested										Median Reactivity
		TTP 007	TTP 008	TTP 012	TTP 017	TTP 030	TTP 041	TTP 042	TTP 049	TTP 052	TTP 058	
CHO	WT full-length (R F R Y Y)	100%	100%	100%	100%	100%	100%	100%	100%	100%	100%	100%
	Mutant K Y K F F (GoF)	63%	119%	100%	76%	67%	78%	72%	72%	102%	84%	77%
	No Protein Supernatant	0%	0%	0%	0%	0%	0%	0%	0%	0%	0%	0%
HEK293	WT full-length (R F R Y Y)	100%	100%	100%	100%	100%	100%	100%	100%	100%	100%	100%
	Mutant K Y K F F (GoF)	72%	93%	90%	65%	74%	70%	84%	78%	100%	87%	81%
	No Protein Supernatant	0%	0%	0%	0%	0%	0%	0%	0%	0%	0%	0%
Dilution Factor for each patient (fold dilution)		80x	200x	60x	40x	30x	40x	40x	30x	400x	60x	
Autoantibodies titer (I.U./mL)		100	120	260	85	59	69	69	52	175	>100	

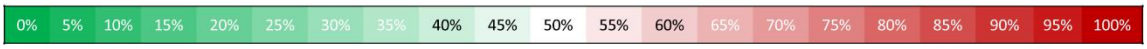

mutant variant II-1 equivalents / full-length WT II-1 equivalents (%)

E

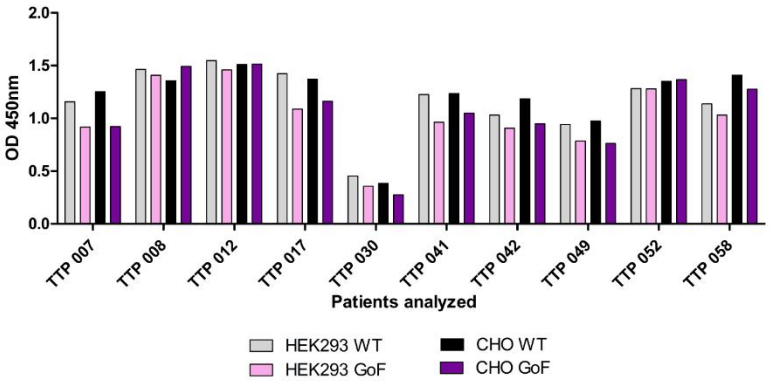

Supplementary Figure S7.